Iterative Learning Controller for Flyback Inverter: A Hybrid Learning Scheme

Minsung Kim, Byeongcheol Han, Sungho Son, Sooa Kim,
Jun-Seok Kim, Kwang-Seop Kim, and Hyosin Kim
Pohang University of Science and Technology, Pohang, Gyeongbuk, South Korea
Email: minsung.kim@postech.ac.kr

***Abstract*—We propose an iterative learning controller (ILC) with hybrid learning scheme for a flyback inverter operating in continuous conduction mode (CCM). The flyback CCM inverter has advantages such as buck-boost capability, small number of circuit components and high power conversion efficiency, making it suitable for the distributed renewable energy systems. But the conventional proportional-integral (PI) controller for the flyback CCM inverter exhibits poor steady-state response because it suffers from control problems caused by right-half-plane (RHP) zero in closed-loop transfer function and time-varying grid-voltage disturbances. Phase-lead ILC is one of the candidates to solve these problems, but it requires massive amounts of memory. To overcome this problem, we use a sampled-data iterative learning controller with phase-lead compensation, in which sampled-data technique reduces the memory space needed. The proposed ILC is also computationally simple and easy to implement. The stability of the closed-loop system is derived and the zero tracking error is achieved. Experimental tests demonstrate the proposed control approach.**

***Index Terms*—unfolding-type inverter, continuous conduction mode, phase-lead compensation, sampled-data technique.**

I. Introduction

Recently, the unfolding-type flyback topology with unfolding circuitry has attracted attention as one of the practical approaches for the microinverter due to its low cost, compact size and high power conversion efficiency [1–9]. Among two operating modes of the flyback inverter such that discontinuous conduction mode (DCM) and continuous conduction mode (CCM), flyback inverter in CCM operation exhibits superior charicteristics in efficiency, voltage stress, current stress and filter design. However, it suffers from control problems caused by right-half-plane (RHP) zero in closed-loop transfer function and time-varying grid-voltage disturbances [10–14]. These problems limit the practical usage of the flyback CCM inverter.

To solve aforementioned problems, a phase-lead iterative learning controller (ILC) was adopted to the flyback inverter [15–19]. This control method observes periodic output signals for one period, leads the phase of these signals, and then uses them to generate the control signals for the next period. Therefore, it provides an outstanding trajectory tracking and disturbance elimination in the periodic control tasks. But, the phase-lead ILC requires massive amounts of memory to store the output signals and control signals. This aspect increases the development cost of the flyback inverter.

In this paper, we propose a sampled-data ILC with phase-lead compensation for flyback inverter. Sampled-data technique is adopted to achieve accurate tracking performance with low memory requirements. The conventional proportional feedback controller and the duty-ratio feedforward controller are also used with proposed controller to improve the output current tracking performance and to reduce the burden from the feedback controller. Proposed control scheme is computationally simple, easy to implement, and requires low memory space. We conducted experimental tests using the 200-W AC module prototype to demonstrate its validity.

The remainder of this study is organized as follows. In Section II, modelling of the flyback CCM inverter is introduced. In Section III, the proposed control scheme is presented and the error convergence of the closed-loop system is proved. In Section IV, the simulation and experimental results are presented. Finally, conclusions are drawn in Section V.

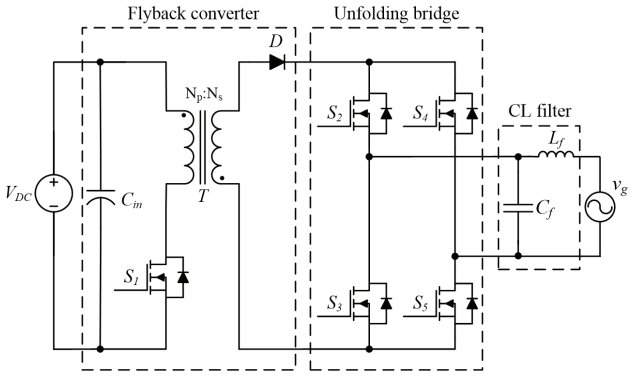

Fig. 1. Circuit diagram of the unfolding-type flyback inverter.

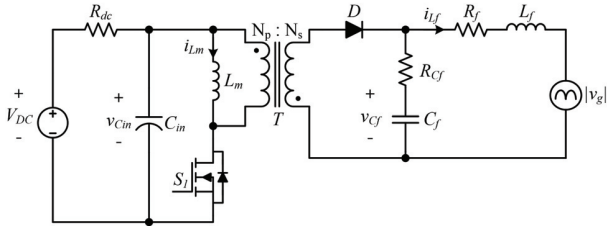

Fig. 2. Equivalent circuit of the unfolding-type flyback inverter.

II. System modelling of the converter

A. Operation of the flyback CCM inverter

The circuit diagram of the unfolding-type flyback inverter is described in Fig. 1. It is composed of input capacitor C_{in}, primary switch S_1, diode D, transformer T with turns ratio $n = N_s/N_p$, an unfolding bridge (S_2-S_5), and a capacitor-inductor (C_f,L_f) output filter.

The equivalent circuit of the flyback CCM inverter is shown in Fig. 2. i_{L_m} is the current that flows through the magnetizing inductor L_m, i_{pri} and i_{sec} are respectively the primary and secondary current of the transformer. The parasitic components are presented as the series resistance R_f of the output filter inductor L_f and R_{C_f} of the output filter capacitor C_f.

B. Dynamic model of the flyback CCM inverter

The flyback CCM inverter experiences two phases: 1) S_1 turned on and D turned off; 2) S_1 turned off and D turned on. The state equations in phases 1 and 2 are represented as follows:

Phase 1 (S_1 on, D off):

$$\begin{bmatrix} \frac{di_{L_m}(t)}{dt} \\ \frac{dv_{C_{in}}(t)}{dt} \\ \frac{di_{L_f}(t)}{dt} \\ \frac{dv_{C_f}(t)}{dt} \end{bmatrix} = \begin{bmatrix} 0 & \frac{1}{L_m} & 0 & 0 \\ -\frac{1}{C_{in}} & -\frac{1}{R_{dc}C_{in}} & 0 & 0 \\ 0 & 0 & -\frac{R_{C_f}+R_f}{L_f} & \frac{1}{L_f} \\ 0 & 0 & -\frac{1}{C_f} & 0 \end{bmatrix} \begin{bmatrix} i_{L_m}(t) \\ v_{C_{in}}(t) \\ i_{L_f}(t) \\ v_{C_f}(t) \end{bmatrix} + \begin{bmatrix} 0 & 0 \\ \frac{1}{R_{dc}C_{in}} & 0 \\ 0 & -\frac{1}{L_f} \\ 0 & 0 \end{bmatrix} \begin{bmatrix} V_{DC} \\ |v_g(t)| \end{bmatrix}, \tag{1}$$

Phase 2 (S_1 off, D on):

$$\begin{bmatrix} \frac{di_{L_m}(t)}{dt} \\ \frac{dv_{C_{in}}(t)}{dt} \\ \frac{di_{L_f}(t)}{dt} \\ \frac{dv_{C_f}(t)}{dt} \end{bmatrix} = \begin{bmatrix} -\frac{R_{C_f}}{n^2L_m} & 0 & \frac{R_{C_f}}{nL_m} & -\frac{1}{nL_m} \\ 0 & -\frac{1}{R_{dc}C_{in}} & 0 & 0 \\ \frac{R_{C_f}}{nL_f} & 0 & -\frac{R_{C_f}+R_f}{L_f} & \frac{1}{L_f} \\ \frac{1}{nC_f} & 0 & -\frac{1}{C_f} & 0 \end{bmatrix} \begin{bmatrix} i_{L_m}(t) \\ v_{C_{in}}(t) \\ i_{L_f}(t) \\ v_{C_f}(t) \end{bmatrix} + \begin{bmatrix} 0 & 0 \\ \frac{1}{R_{dc}C_{in}} & 0 \\ 0 & -\frac{1}{L_f} \\ 0 & 0 \end{bmatrix} \begin{bmatrix} V_{DC} \\ |v_g(t)| \end{bmatrix}. \tag{2}$$

By averaging state-space model, we can derive the average model as

$$\begin{bmatrix} \frac{di_{L_m}(t)}{dt} \\ \frac{dv_{C_{in}}(t)}{dt} \\ \frac{di_{L_f}(t)}{dt} \\ \frac{dv_{C_f}(t)}{dt} \end{bmatrix} = \begin{bmatrix} -\frac{R_{C_f}d_2(t)}{n^2L_m} & \frac{d_1(t)}{L_m} & \frac{R_{C_f}d_2(t)}{nL_m} & -\frac{d_2(t)}{nL_m} \\ -\frac{d_1(t)}{C_{in}} & -\frac{1}{R_{dc}C_{in}} & 0 & 0 \\ \frac{R_{C_f}d_2(t)}{nL_f} & 0 & -\frac{R_{C_f}+R_f}{L_f} & \frac{1}{L_f} \\ \frac{d_2(t)}{nC_f} & 0 & -\frac{1}{C_f} & 0 \end{bmatrix} \begin{bmatrix} i_{L_m}(t) \\ v_{C_{in}}(t) \\ i_{L_f}(t) \\ v_{C_f}(t) \end{bmatrix} + \begin{bmatrix} 0 & 0 \\ \frac{1}{R_{dc}C_{in}} & 0 \\ 0 & -\frac{1}{L_f} \\ 0 & 0 \end{bmatrix} \begin{bmatrix} V_{DC} \\ |v_g(t)| \end{bmatrix}, \tag{3}$$

$$y(t) = \begin{bmatrix} 0 & 0 & 1 & 0 \end{bmatrix} \begin{bmatrix} i_{L_m}(t) \\ v_{C_{in}}(t) \\ i_{L_f}(t) \\ v_{C_f}(t) \end{bmatrix}, \tag{4}$$

where $d_1(t)$ is the duty ratio when the switch is turned on and $d_2(t) = 1 - d_1(t)$.

By linearizing (3) and (4), we are able to formulate the small signal model as follows:

$$\dot{\mathbf{x}}(t) = A\mathbf{x}(t) + Bd(t), \tag{5}$$

$$y(t) = C\mathbf{x}(t). \tag{6}$$

where $\mathbf{x}(t) = [\tilde{i}_{L_m}(t), \tilde{v}_{C_{in}}(t), \tilde{i}_{L_f}(t), \tilde{v}_{C_f}(t)]^T$, $d(t) = \tilde{d}_1(t)$, $y(t) = \tilde{i}_{L_f}(t)$ are the state vector, the control input, and the output. $\tilde{i}_{L_m}(t)$, $\tilde{v}_{C_{in}}(t)$, $\tilde{i}_{L_f}(t)$, $\tilde{v}_{C_f}(t)$ and $\tilde{d}_1(t)$ are incremental variations of $i_{L_m}(t)$, $v_{C_{in}}(t)$, $i_{L_f}(t)$, $v_{C_f}(t)$ and $d_1(t)$. Parameters A, B and C are determined as

$$A = \begin{bmatrix} \frac{R_{c_f}(1-D)}{n^2L_m^2} & \frac{D}{L_m} & \frac{R_{c_f}(1-D)}{nL_m} & -\frac{1-D}{nL_m} \\ -\frac{D}{C_{in}} & -\frac{1}{R_{dc}C_{in}} & 0 & 0 \\ \frac{R_{c_f}(1-D)}{nL_f} & 0 & -\frac{R_{c_f}+R_f}{L_f} & \frac{1}{L_f} \\ \frac{1-D}{nC_f} & 0 & -\frac{1}{C_f} & 0 \end{bmatrix}, \tag{7}$$

$$B = \begin{bmatrix} \frac{R_{c_f}I_{L_m}}{n^2L_m} + \frac{V_{C_{in}}}{L_m} - \frac{R_{c_f}I_{L_f}-V_{C_f}}{nL_m} \\ -\frac{I_{L_m}}{C_{dc}} \\ -\frac{R_{c_f}I_{L_m}}{nL_f} \\ -\frac{I_{L_m}}{nC_f} \end{bmatrix}, \tag{8}$$

$$C = \begin{bmatrix} 0 & 0 & 1 & 0 \end{bmatrix}, \tag{9}$$

where I_{L_m}, $V_{C_{in}}$, I_{L_f}, V_{C_f} and D are the operating points of $i_{L_m}(t)$, $v_{C_{in}}(t)$, $i_{L_f}(t)$, $v_{C_f}(t)$ and $d_1(t)$. Since the flyback inverter performs the same tasks repetitively with a grid period T_g, it can be described as a series of iterative linear systems:

$$\dot{\mathbf{x}}_i(t) = A\mathbf{x}_i(t) + Bd_i(t), \tag{10}$$

$$y_i(t) = C\mathbf{x}_i(t), \tag{11}$$

where i indicates the number of iterations, $\mathbf{x}_i(t)$, $y_i(t)$ and $d_i(t)$ are respectively the state vector, the output and the input at the ith iteration.

Then, discretizing the equations (10)-(11) yields a series of discrete-time iterative linear systems:

$$\mathbf{x}_i(k+1) = F\mathbf{x}_i(k) + Gu_c(k), \tag{12}$$

$$y_i(k) = H\mathbf{x}_i(k). \tag{13}$$

where k is the discrete time index starting from $k = 0$ to $k = k_T$, $\mathbf{x}_i(k) \in R^{4\times1}$, $y_i(k) \in R$ and $u_c(k) \in R$ are respectively

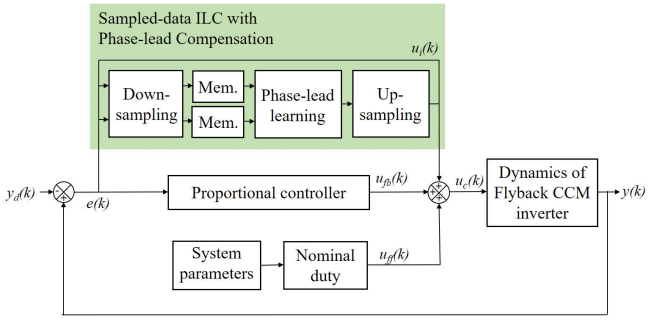

Fig. 3. Schematic diagram of the proposed control scheme.

the state vector, the system output and the control input for $i = 1, 2, ...$, and $F \in R^{4\times4}, G \in R^{4\times1}$ and $H \in R^{1\times4}$ are the discrete-time system matrices.

The proposed controller is then developed based on the following assumptions.

Assumption 1. The desired system is invertible, that is, given a desired output trajectory $y_d(k)$ there exists a unique bounded input trajectory $u_d(k)$ such that

$$\mathbf{x_d}(k+1) = F\mathbf{x_d}(k) + Gu_d(k), \tag{14}$$

$$y_d(k) = H\mathbf{x_d}(k) \quad \text{for all } k \in [0, k_T], \tag{15}$$

where $\mathbf{x_d}(k) \in R^{4\times1}$ is the desired state vector.

Assumption 2. The initial resetting condition is satisfied for all iterations, i.e., $\mathbf{x}_i(0) = \mathbf{x_d}(0)$ and $y_i(0) = y_d(0)$, $i = 1, 2, ...$.

III. Controller Scheme

A. Proposed ILC and stability analysis

The proposed control input consists of

$$u_c(k) = u_{fb}(k) + u_{ff}(k) + u_i(k), \tag{16}$$

where $u_{fb}(k) \in R$ is the state-feedback controller, $u_{ff}(k) \in R$ is the nominal duty, and $u_i(k) \in R$ is the proposed iterative learning controller. For $u_{fb}(k)$, $u_{ff}(k)$, $u_i(k)$, we propose to use

$$u_{fb}(k) = k_p e(k), \tag{17}$$

$$u_{ff}(k) = D_{no}(k) = \frac{|v_g(t)|}{nV_{DC} + |v_g(t)|}, \tag{18}$$

$$u_{i+1}(k) = \begin{cases} u_i(k) + k_l e_i(k+\lambda m), & \text{if } mod(k,m) = 0 \\ u_{i+1}(k-1), & \text{else.} \end{cases} \tag{19}$$

where k_p is the proportional gain; $m \geq 1$ is the ratio between the sampling frequency and the control frequency of ILC; $e_i(k) = y_d(k) - y_i(k)$ is the output error; k_l is the learning controller gain; $i = 0, 1, ...$ is the iteration index; $k = 0, ..., k_T$ is the discrete-time index. $mod(k, m)$ is the remainder when k is divided by m. λ is the phase-lead step.

In the proposed controller, the control frequency of ILC is slower than that of the feedback controller and the nominal duty. This method is called the sampling-data technique [20].

The sampled-data input, state, output and desired output are respectively represented as:

$$[u_{i,s}(0), u_{i,s}(1), ..., u_{i,s}(k_N - 1)] = [u_i(0), u_i(m), ..., u_i((k_N - 1)m)], \tag{20}$$

$$[x_{i,s}(1), x_{i,s}(2), ..., x_{i,s}(k_N)] = [x_i(m), x_i(2m), ..., x_i(k_N m)], \tag{21}$$

$$[y_{i,s}(1), y_{i,s}(2), ..., y_{i,s}(k_N)] = [y_i(m), y_i(2m), ..., y_i(k_N m)], \tag{22}$$

$$[y_{d,s}(1), y_{d,s}(2), ..., y_{d,s}(k_N)] = [y_d(m), y_d(2m), ..., y_d(k_N m)], \tag{23}$$

where the subscript s denotes the sampled-data signal and k_N is the quotient when k_T is divided by m.

Theorem 1. Consider the discrete-time iterative linear system (12) and (13). Assume that the assumption 1 and 2 are satisfied and that the inequality

$$\rho(I - k_l PL) < 1 \tag{24}$$

holds, where I is the $k_N \times k_N$ identity matrix, and $P \in R^{k_N \times k_N}$, $L \in R^{k_N \times k_N}$ are represented as:

$$P = \begin{bmatrix} HG_s & 0 & \cdots & 0 \\ HF_sG_s & HG_s & \cdots & 0 \\ \vdots & \vdots & \ddots & \vdots \\ HF_s^{k_N-1}G_s & HF_s^{k_N-2}G_s & \cdots & HG_s \end{bmatrix}, \tag{25}$$

$$L = \begin{bmatrix} l_{1,1} & l_{1,2} & \cdots & l_{1,k_N} \\ l_{2,1} & l_{2,2} & \cdots & l_{2,k_N} \\ \vdots & \vdots & \ddots & \vdots \\ l_{k_N,1} & l_{k_N,2} & \cdots & l_{k_N,k_N} \end{bmatrix}, \tag{26}$$

where

$$F_s = (F - k_p GH)^m, \tag{27}$$

$$G_s = \sum_{j=0}^{m-1} (F - k_p GH)^{m-1-j} G, \tag{28}$$

$$l_{p,q} = \begin{cases} 1, \text{ if } p + \lambda - 1 = q \\ 0, \text{ else} \end{cases} \qquad p, q = 1, ..., k_N. \tag{29}$$

Then, the proposed controller (16) guarantees that the output tracking error of the closed loop system converges to zero.

Proof. Applying the controller (16) to the discrete-time iterative linear system (12) and substituting the proportional control law (17) into the resulting equation yields

$$\begin{aligned} &\mathbf{x}_i(k+1) \\ &= F\mathbf{x}_i(k) + G(u_{fb}(k) + u_{ff}(k) + u_i(k)) \\ &= F\mathbf{x}_i(k) + G(k_p e_i(k) + u_{ff}(k) + u_i(k)) \\ &= F\mathbf{x}_i(k) + G(k_p(y_d(k) - H\mathbf{x}_i(k)) + u_{ff}(k) + u_i(k)) \\ &= (F - k_p GH)\mathbf{x}_i(k) + Gu_i(k) + G(k_p y_d(k) + u_{ff}(k)). \end{aligned} \tag{30}$$

Substituting the discrete-time index $k = 0, 1, ..., m-1$ into (30), we have

$$\mathbf{x}_i(1) = (F - k_p GH)\mathbf{x}_i(0) + Gu_i(0) + G(k_p y_d(0) + u_{ff}(0)), \tag{31}$$

$$\begin{aligned}\mathbf{x}_i(2) = &(F - k_p GH)^2 \mathbf{x}_i(0) + (F - k_p GH)Gu_i(0) + Gu_i(1) \\ &+ (F - k_p GH)G(k_p y_d(0) + u_{ff}(0)) \\ &+ G(k_p y_d(1) + u_{ff}(1)),\end{aligned} \tag{32}$$

$$\vdots$$

$$\begin{aligned}\mathbf{x}_i(m) = &(F - k_p GH)^m \mathbf{x}_i(0) + (F - k_p GH)^{m-1} Gu_i(0) \\ &+ \cdots + Gu_i(m-1) \\ &+ (F - k_p GH)^{m-1} G(k_p y_d(0) + u_{ff}(0)) \\ &+ \cdots + G(k_p y_d(m-1) + u_{ff}(m-1)).\end{aligned} \tag{33}$$

Since the ILC inputs $u_i(k)$ are the same as $u_i(0)$ for all $k \in [0, m-1]$ as in (19), we can rewrite (33) as

$$\begin{aligned}\mathbf{x}_i(m) &= (F - k_p GH)^m \mathbf{x}_i(0) + \sum_{j=0}^{m-1} (F - k_p GH)^{m-1-j} Gu_i(0) \\ &\quad + \sum_{j=0}^{m-1} (F - k_p GH)^{m-1-j} G(k_p y_d(j) + u_{ff}(j)) \\ &= F_s \mathbf{x}_i(0) + G_s u_{i,s}(0) + w(0).\end{aligned} \tag{34}$$

where $w(0) = \sum_{j=0}^{m-1} (F - k_p GH)^{m-1-j} G(k_p y_d(j) + u_{ff}(j))$. Applying the same steps for all sampled-data states, we obtain the sampled-data linear system as

$$\mathbf{x}_{i,s}(n+1) = F_s \mathbf{x}_{i,s}(n) + G_s u_{i,s}(n) + w(n), \tag{35}$$

$$y_{i,s}(n) = H\mathbf{x}_{i,s}(n), \text{ for all } n \in [0, k_N], \tag{36}$$

where

$$w(n) = \sum_{j=nm}^{(n+1)m-1} (F - k_p GH)^{(n+1)m-1-j} G(k_p y_d(j) + u_{ff}(j)). \tag{37}$$

Note here that $w(n)$ is the sum of the desired output and the feedforward input for $n = 0, 1, ..., k_N - 1$. It means that $w(n)$ is iteration-invariant. Solving the sampled-data linear system (35) and (36) yields

$$\begin{aligned}y_{i,s}(n) = &HF_s^n \mathbf{x}_{i,s}(0) + \sum_{l=0}^{n-1} HF_s^{n-1-l} G_s u_{i,s}(l) \\ &+ \sum_{l=0}^{n-1} HF_s^{n-1-l} w(l).\end{aligned} \tag{38}$$

Let us define the output error $e_{i,s}(n) = y_{d,s}(n) - y_{i,s}(n)$. Subtracting the output errors at the ith iteration from those at the $(i+1)$th iteration, we obtain

$$\begin{aligned}&e_{i+1,s}(n) - e_{i,s}(n) \\ &= y_{i,s}(n) - y_{i+1,s}(n) \\ &= HF_s^n(\mathbf{x}_{i,s}(0) - \mathbf{x}_{i+1,s}(0)) \\ &\quad + \sum_{l=0}^{n-1} HF_s^{n-1-l} G_s(u_{i,s}(l) - u_{i+1,s}(l)).\end{aligned} \tag{39}$$

Applying assumption 2 and the ILC control law (19) to (39), we have

$$\begin{aligned}&e_{i+1,s}(n) - e_{i,s}(n) \\ &= HF_s^n(\mathbf{x}_{i,s}(0) - \mathbf{x}_{i+1,s}(0)) \\ &\quad + \sum_{l=0}^{n-1} HF_s^{n-1-l} G_s(u_{i,s}(l) - u_{i+1,s}(l)) \\ &= -k_l \sum_{l=0}^{n-1} HF_s^{n-1-l} G_s e_{i,s}(l+\lambda).\end{aligned} \tag{40}$$

Converting (40) into the matrix form yields

$$E_{i+1,s} = (I - k_l PL)E_{i,s}, \tag{41}$$

where $E_{i,s} = [e_{i,s}(1), e_{i,s}(2), ..., e_{i,s}(k_N)]^T$. So if the condition (24) is satisfied, then all the eigenvalues of $I - k_l PL$ exist within the unit circle, and consequently the error converges to zero. ■

TABLE I
PARAMETERS AND OPERATING CONDITIONS OF THE FLYBACK INVERTER

Parameters	Symbols	Value
Transformer turn ratio	n	3.5
Magnetizing inductance	L_m	160 uH
Leakage inductance	L_{lk}	2.4 uH
Filter inductance	L_f	1.0 mH
Input capacitance	C_{in}	2.0 mF
Filter capacitance	C_f	0.1 uF
Input resistance	R_{dc}	1 Ω
Resistance in filter capacitor	R_{cf}	0.48 Ω
Resistance in filter inductor	R_f	0.28 Ω
Operating conditions	**Symbols**	**Value**
Nominal voltage of source	V_{dc}	60 V
Grid voltage	v_g	220 V_{rms}
Grid frequency	f_g	60 Hz
Rated power of source	P_o	200 W
Switching frequency	f_s	50 kHz
Sampling frequency	f_c	50 kHz

IV. EXPERIMENTAL RESULTS

The proposed control scheme was evaluated by the experiment using the prototype of the flyback CCM inverter. Table I shows the circuit parameters and the operating conditions used both experimental test. The control algorithm is implemented on a TMS320F28377 microcontroller. Proportional control gain k_p was set to 0.05 and the nominal duty value was determined using the parameters given in Table I.

A. Experimental results

Fig. 4 shows the experimental results of the flyback CCM inverter when the proposed control scheme is applied. We used the output power $P_o = 100$ W, the forgetting factor $\gamma = 0.01$, phase-lead step $\lambda = 2$, and sampled-data ratio $m = 3$ for the experiment.

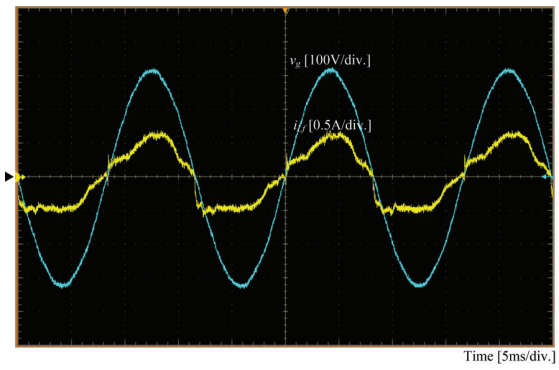

(a)

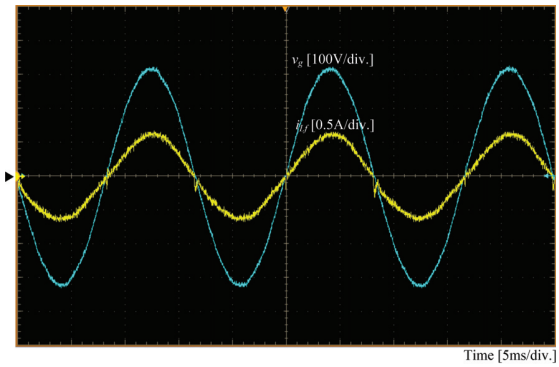

(b)

Fig. 4. Waveforms of the grid voltage (red) and the output current (blue) when the output power is set to 100 W. (a) PI controller. (b) Proposed ILC.

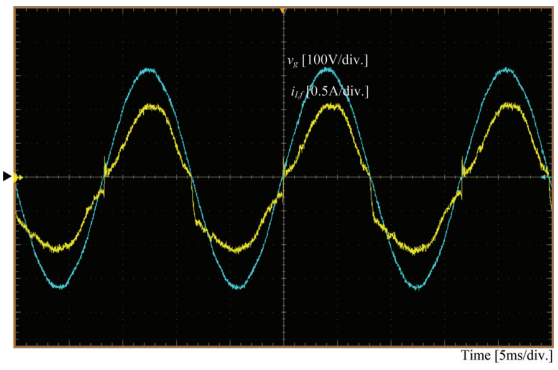

(a)

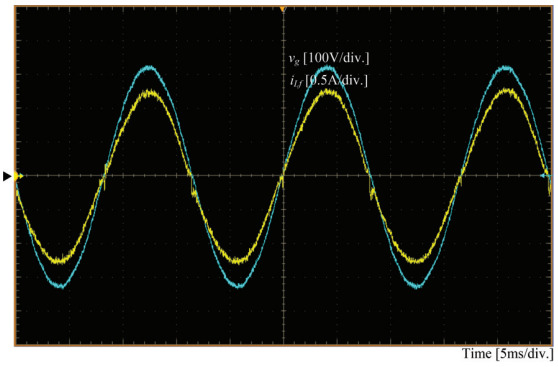

(b)

Fig. 5. Waveforms of the grid voltage (red) and the output current (blue) when the output power is set to 200 W. (a) PI controller. (b) Proposed ILC.

When the PI control plus nominal duty is applied to the proposed converter, the output current was highly distorted (Fig. 4(a)). When the proposed ILC is used, the output current tracks the reference output current well only using one-third of the memory required in ILC with phase-lead compensator (Fig. 4(b)).

We also tested the conventional and proposed controller when the output power was set to $P_o = 200$ W. Similar to Fig. 4(a), the output current is highly disturbed (Fig. 5(a)). Similar to Fig. 4(b), the proposed control scheme performs properly (Fig. 5(b)).

V. Conclusion

In this paper, we propose a sampled-data iterative learning control scheme with phase-lead compensation for the flyback CCM inverter. The use of phase-lead ILC itself would achieve desirable steady-state response of the flyback CCM inverter, but it requires massive amounts of memory. In the proposed ILC scheme, a sampled-data technique has been used to reduce the amount of required memory. The stability of the closed-loop system is derived and the zero tracking error is achieved. Even with a small amount of memory, experimental results shows that the control accuracy was satisfactory.

Acknowledgment

This research was supported by the MSIP (Ministry of Science, ICT and Future Planning), Korea, under the "ICT Consilience Creative Program" (IITP-R0346-16-1007) supervised by the IITP (Institute for Information & communications Technology Promotion) and in part by the National Research Foundation of Korea (NRF) grant funded by MSIP (No. 2017R1C1B1003084).

References

[1] H. Hu, S. Harb, N. H. Kutkut, Z. J. Shen, and I. Batarseh, "A single-stage microinverter without using eletrolytic capacitors," *IEEE Trans. Power Electron.*, vol. 28, no. 6, pp. 2677-2687, 2013.

[2] M. Gao, M. Chen, C. Zhang, and Z. Qian, "Analysis and implementation of an improved flyback inverter for photovoltaic ac module applications," *IEEE Trans. Power Electron.*, vol. 29, no. 7, pp. 3428-3444, 2014.

[3] N. Sukesh, M. Pahlevaninezhad, and P. K. Jain, "Analysis and implementation of a single-stage flyback PV microinverter with soft switching," *IEEE Trans. on Ind. Electron.*, vol. 61, no. 4, pp. 1819-1833, 2014.

[4] B. Tamyurek and B. Kirimer, "An interleaved high-power flyback inverter for photovoltaic applications," *IEEE Trans. Power Electron.*, vol. 30, no. 6, pp. 3228-3241, 2015.

[5] F. Karbakhsh, M. Amiri, and H. A. Zarchi, "Two-switch flyback inverter employing a current sensorless MPPT and scalar control for low cost solar powered pumps," *IET Renew. Power Gen.*, vol. 11, no. 5, pp. 669-677, 2016.

[6] G. C. Christidis, A. C. Nanakos, and E. C. Tatakis, "Hybrid discontinuous/boundary conduction mode of flyback microinverter for ACPV modules," *IEEE Trans. Power Electron.*, vol. 31, no. 6, pp. 4195-4205, 2016.

[7] H. A. Sher, A. A. Rizvi, K. E. Addoweesh, and K. Al-Haddad, "A single-stage stand-alone photovoltaic energy system with high tracking efficiency," *IEEE Trans. Sustain. Energy.*, vol. 8, no. 2, pp. 755-762, 2017.

[8] M. H. Zare, M. Mohamadian, and R. Beiranvand, "A single-phase grid-connected photovoltaic inverter based on a three-switch three-port flyback with series power decoupling circuit," *IEEE Trans. on Ind. Electron.*, vol. 64, no. 3, pp. 2062-2071, 2017.

[9] K. S. Kim, S. H. Lee, W. J. Cha, J. M. Kwon, and B. H. Kwon, "Bidirectional single power-conversion DCAC converter with noncomplementary active-clamp circuits," *IEEE Trans. on Ind. Electron.*, vol. 63, no. 8, pp. 4860-4867, 2016.

[10] Y. Li, and R. Oruganti, "A low cost flyback CCM inverter for AC module application," *IEEE Trans. Power Electron.*, vol. 27, no. 3, pp. 1295-1303, 2012.

[11] F. F. Edwin, W. Xiao, and V. Khadkikar, "Dynamic modeling and control of interleaved flyback module-integrated converter for PV power applications," *IEEE Trans. on Ind. Electron.*, vol. 61, no. 3, pp. 1377-1388, 2014.

[12] S. H. Lee, W. J. Cha, B. H. Kwon, and M. Kim, "Discrete-time repetitive control of flyback CCM inverter for PV power applications," *IEEE Trans. on Ind. Electron.*, vol. 63, no. 2, pp. 976-984, 2016.

[13] H. Kim and M. Kim, "Duty-ratio feedforward controller design for single-stage flyback CCM inverter," *Electron. Lett.*, vol. 52, no. 25, pp. 2053-2055, 2016.

[14] S. M. Wi, J. S. Lee, and M. Kim, "Exponentially Stable Lyapunov Function Based Controller for Flyback CCM Converter," *IEEE Trans. on Ind. Electron.* (Accepted for publication, DOI: 10.1109/TIE.2017.2733459)

[15] B. Zhang, K. Zhou, Y. Wang, and D. Wang, "Performance improvement of repetitive controlled PWM inverters: A phaselead compensation solution," *International J. Circ. Theor. App.*, vol. 38, no. 5, pp. 453-469, 2010.

[16] Q. Zhao and Y. Ye, "Fractional phase lead compensation RC for an inverter: analysis, design, and verification," *IEEE Trans. on Ind. Electron.*, vol. 64, no. 4, pp. 3127-3136, 2017.

[17] Z. Liu, B. Zhang, and K. Zhou, "Universal fractional-order design of linear phase lead compensation multi rate repetitive control for PWM inverters," *IEEE Trans. on Ind. Electron.*, 2017.

[18] H. Kim, J. S. Lee, J. S. Lai, and Kim, M. "Iterative learning controller with multiple phase-lead compensation for dual-mode flyback inverter," *IEEE Trans. Power Electron.*, vol. 32, no. 8, pp. 6468-6480, 2017.

[19] B. Han, J. S. Lee, and M. Kim, "Repetitive controller with phase-lead compensation for Cuk CCM inverter," *IEEE Trans. on Ind. Electron.* (Accepted for publication, DOI: 10.1109/TIE.2017.2739678)

[20] B. Zhang, D. Wang, Y. Ye, K. Zhou, and Y. Wang, "Cyclic pseudo-downsampled iterative learning control for high performance tracking," *Control Eng Pract.*, vol. 17, no. 8, pp. 957-965, 2009.